COMMUNICATION

Operando 3D Visualization of Migration and Degradation of Pt Cathode Catalyst in a Polymer Electrolyte Fuel Cell**

Hirosuke Matsui*, Nozomu Ishiguro, Tomoya Uruga, Oki Sekizawa, Kotaro Higashi, Naoyuki Maejima, and Mizuki Tada*

Abstract: *The three-dimensional (3D) distribution and oxidation state of a Pt cathode catalyst in a practical membrane electrode assembly (MEA) were visualized in a practical polymer electrolyte fuel cell (PEFC) under fuel-cell operating conditions. Operando 3D computed-tomography imaging with X-ray absorption near edge structure (XANES) spectroscopy (CT-XANES) clearly revealed the heterogeneous migration and degradation of Pt cathode catalyst in an MEA during accelerated degradation test (ADT) of PEFC. The degradative Pt migration proceeded over the entire cathode catalyst layer and spread to MEA depth direction into the Nafion membrane.*

Polymer electrolyte fuel cell (PEFC) is promising as a sustainable power source, and its use in automobiles has been investigated worldwide.[1] For practical applications and commercialization of PEFC, it is essential to improve the durability of a cathode catalyst, which is usually Pt/C, in a membrane electrode assembly (MEA). The cathode catalyst in MEA is exposed to acidic conditions, and repeated voltage cycling causes severe oxidative dissolution and subsequent aggregation of the cathode catalyst, resulting in the deactivation and degradation of MEA.[2]

There are several approaches to identify major factors in catalyst degradation in MEA, such as electrochemical analysis[3], electron microscopy[4], spectroscopic techniques[5], and theoretical calculations[6]. The mechanism of the dissolution of Pt cathode catalysts has been discussed[7], and the repetition of catalyst oxidation often causes the irreversible dissolution and formation of large aggregates of Pt catalyst particles at cathode.[8] The degradation of the cathode catalyst occurs throughout MEA, but there was no report to reveal the three-dimensional (3D) heterogeneous catalyst degradation in MEA under PEFC operating conditions.

Recently, 3D imaging techniques using X-rays as a probe have been developed to visualize heterogeneous structures in practical materials in real space.[9] Computed tomography (CT), which is an effective method for reconstructing 3D images of a sample from a series of transmission images, can be measured with a hard X-ray probe. A sample is rotated around an axis perpendicular to incident X-ray beam, and a series of X-ray transmission images are recorded. The high transmission of hard X-rays enables the measurement of the positions of Pt catalysts in a PEFC cell with lots of water and gases, and combining this reconstruction technique with X-ray absorption fine structure spectroscopy provides a practical technique to visualize the 3D degradation of the cathode catalyst in MEA under PEFC operating conditions.

We have reported the *ex situ* imaging of Pt cathode catalyst layers in MEAs by X-ray computed laminography X-ray absorption near edge structure (XANES).[10] In laminography, a sample is inclined to an incident X-ray beam to collect a data set of transmission images from each projection angle, and the 3D distributions of a Pt catalyst in as-prepared and degraded MEAs taken from PEFC cells were imaged. However, it was difficult to conduct *in situ* laminography measurement under PEFC operating conditions due to PEFC cell design having wide X-ray windows[11], and there have been no reports on *in situ* 3D visualization of Pt catalyst in MEA in a practical PEFC system.

In this paper, we report the 3D visualization of the location and oxidation state of a Pt cathode catalyst in an MEA by *operando* CT-XANES under PEFC operating conditions. The reconstruction and analysis of CT-XANES data provided the distribution and oxidation state of the Pt catalyst at each position in the MEA. The *operando* CT-XANES measurements were conducted before and after the cycles of typical accelerated degradation test (ADT) for PEFC, and the migration and degradation of the Pt cathode catalyst in the MEA were successfully visualized for the first time.

An MEA with a Pt/C cathode catalyst (0.5 $mg_{\text{-Pt}}$ cm^{-2}) and a Pd/C anode catalyst (0.5 $mg_{\text{-Pd}}$ cm^{-2}) was enclosed in a PEFC cell designed for CT-XANES measurements (Figure S1). The thicknesses of components in the MEA were 20 μm (Pt/C cathode catalyst layer), 50 μm (Nafion polymer electrolyte membrane), and 20 μm (Pd/C anode catalyst layer) estimated by a cross-sectional SEM image (Figure S2). At both sides of the MEA, 100-μm-thick gas diffusion layers (GDLs) were inserted. The MEA was aged by typical current steps, and then 20,000 cycles of ADT with rectangular voltage cycling steps (0.6–1.0 V for 3 s) were conducted (Supporting Information 1). Electrochemical active surface area (ECSA) was 72 m^2 $g_{\text{-Pt}}^{-1}$ after the initial aging treatment, and it decreased to 30 m^2 $g_{\text{-Pt}}^{-1}$ after the 20,000 ADT cycles (Figure S3). Series of *operando* CT transmission images at 184 energies around the Pt L_{III}-edge were recorded at 1.0 V before and after ADT (Supporting Information 2, Figure S4).

[*] Dr. H. Matsui, Dr. N. Maejima, Prof. Dr. M. Tada
Department of Chemistry, Graduate School of Science & Research Center for Materials Science (RCMS) & Integrated Research Consortium on Chemical Science (IRCCS), Nagoya University
Furo, Chikusa, Nagoya, Aichi 464-8602 (Japan)
E-mail: mtada@chem.nagoya-u.ac.jp
Dr. N. Ishiguro, Prof. Dr. M. Tada
RIKEN SPring-8 Center, Koto, Sayo, Hyogo 679-5198 (Japan)
Dr. K. Higashi, Dr. O. Sekizawa, Prof. Dr. T. Uruga
Innovation Research Center for Fuel Cells, The University of Electro-Communications, Chofu, Tokyo 182-8585 (Japan)
Dr. T. Uruga
Japan Synchrotron Radiation Research Center, SPring-8
Koto, Sayo, Hyogo 679-5198 (Japan)

[**] This work was supported in part by the NEDO program, the Murata Science Foundation, a JSPS KAKENHI Grant-in-Aid for Scientific Research (B) (26288005), and JSPS KAKENHI Grant-in-Aid for Young Scientists (B) (16K18288). CT-XANES measurements were performed at SPring-8: Nos. 2013B7822, 2014A7821, 2014B7821, 2015A7821, and 2015B7821. SEM was measured at High Voltage Electron Microscope Laboratory, Institute of Materials and Systems for Sustainability, Nagoya University, supported by "Advanced Characterization Nanotechnology Platform" of MEXT, Japan. Supporting information for this article is given via a link at the end of the document.

Changes in the ECSA observed before and after the CT-XANES measurements were negligible (Figure S3).

The reconstruction of Pt L_{III}-edge CT-XANES spectra provided the 3D images of the amounts and valence states of the Pt catalyst in the MEA before and after the ADT cycles. In general, CT requires a sample smaller than the observation field in all projection angles, but the transmission images of the MEA, which is a flat membrane, cannot be measured at all projection angles. We used the angle-limited CT technique[12] with an ordered-subset expectation maximization (OS-EM) method for imaging the MEA (Supporting Information 3).

We reconstructed 3D images of three parameters from the CT-XANES analysis: (**i**) morphology image, (**ii**) Pt distribution image, and (**iii**) Pt valence state image in the MEA. (**i**) was obtained by the reconstruction of CT data measured at 11.497 keV, which was the energy lower than the Pt L_{III}-edge (Figure 1 (**i**)). *X* and *Y* axes corresponded to the in-plane directions of the MEA. *Z* axis was perpendicular to the MEA plane, i.e. the depth direction from the cathode to the anode, the origin of which was set at the interface of the cathode catalyst layer and GDL. The depths at *Z* = -50, 10, 20, 45, and 80 μm corresponded to the center of cathode GDL, the center of the cathode catalyst layer, the interface of the cathode catalyst layer and the Nafion membrane, the center of the Nafion membrane, and the center of the anode catalyst layer, respectively (Figure S2). Differences in the morphology of each component (GDL, catalyst layers, and Nafion membrane) were clearly reconstructed (Figure S5). The total thickness of the MEA on the reconstructed CT image was about 90 μm, which agreed with that on the SEM image (Figure S2). The morphology images before and after ADT demonstrate that the same 3D view area of the MEA was successfully reconstructed by the *operando* CT-XANES during ADT.

Figure 1 (**ii**) shows the 3D reconstructed images of the Pt L_{III}-edge jump, which corresponds to Pt density distribution, in the MEA before and after ADT. The distribution of the Pt catalyst, which is shown in black (low density) to red (high density), was found to be heterogeneous in the cathode catalyst layer. In the cross-sectional image at *Z* = 10 μm, which corresponds to the center of the cathode catalyst layer, the Pt catalyst was present as tiny spots as shown in Figure 1 (**ii**-CS), suggesting that the Pt catalyst was dispersed in the cathode catalyst layer in the MEA before ADT. Red line-like structures (indicated by (a) in Figure 1 (**ii**-CS)) were found in the depth of *Z* = 10 μm. At the interface of the cathode catalyst layer and the Nafion membrane (*Z* = 20 μm), red line-like aggregation was observed at the edge of several domains, suggesting the local aggregation of the Pt catalyst. The contrast of the Pt density at the center of the Nafion membrane (*Z* = 45 μm) was much lower than those at *Z* = 10 and 20 μm (cathode catalyst layer), although some Pt species were observed. The appearance of crack-like structure in the cross-sectional Pt density image at the Nafion membrane implys the limitation of imaging of the Pt distribution in regions with too low Pt density.

The 3D images of the distribution of the Pt catalyst changed greatly after the 20,000 ADT cycles. The fine red spots and lines observed before ADT almost disappeared, and blurred assemblies were entirely observed after ADT (Figure 1 (**ii**)). Severe aggregation was observed in some areas (Figure 1 (**ii**-CS) (b)), whereas the Pt catalyst was lost in other parts ((c) with white-dashed circles). The migration of the Pt cathode catalyst during the ADT cycles was observed for all depths of the cathode catalyst layer.

These images visualized the dissolution of the Pt catalyst to the Nafion membrane attached to the cathode catalyst layer by ADT (Figure 1 (**ii**-CS)). The migration of the Pt catalyst was also observed at the interface of the cathode catalyst layer and the Nafion membrane (*Z* = 20 μm) and in the Nafion membrane (*Z* = 45 μm). The sum of the Pt amounts in the MEA almost unchanged after ADT within the error range of 3%. Hence, it indicates that Pt observed in the Nafion membrane area was caused by the dissolution of the Pt catalyst from the cathode catalyst layer.

To clarify the migration and degradation of the Pt cathode catalyst in the MEA, we visualized the locations of the Pt species in three fractions concerning to the Pt density: **A** (relative Pt density: 0.80-1.00), **B** (0.05-0.80), and **C** (0.00-0.05). The scale

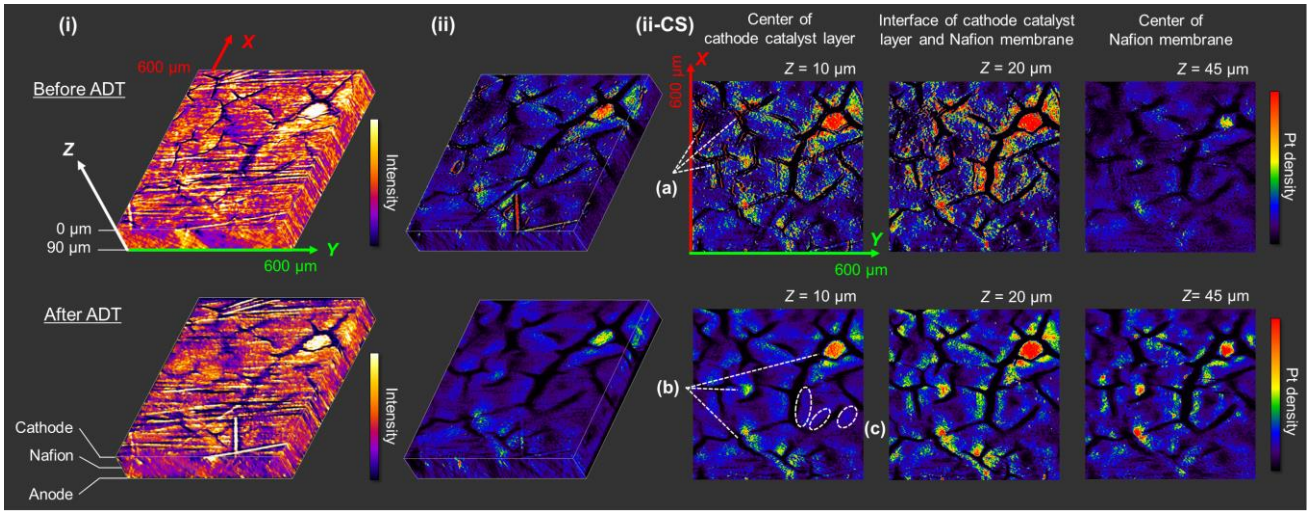

Figure 1. (**i**) 3D images of morphology reconstructed by CT at 11.497 keV. (**ii**) 3D images of the Pt density and (**ii**-CS) their cross-sectional images at *Z* = 10, 20, and 45 μm reconstructed by *in situ* CT-XANES before and after the 20,000 ADT cycles. (a) Observed line-like structures, (b) areas that the Pt catalyst aggregated, and (c) areas that the Pt catalyst was lost (dashed circles).

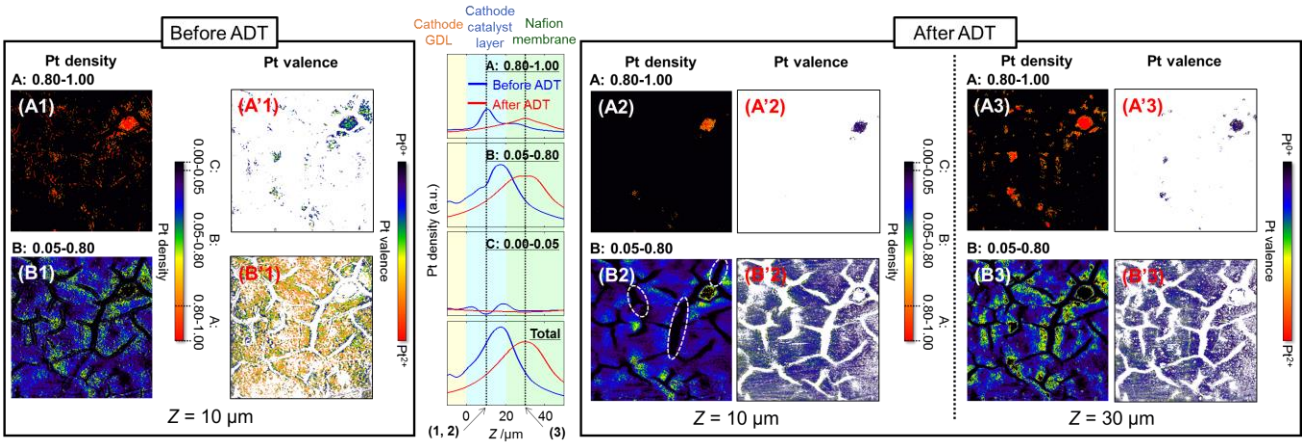

Figure 2. Locations of fractions **A** and **B** in the cross-sectional images of Pt distribution and Pt valence state. (1: before ADT; 2: after the 20,000 ADT cycles) at Z = 10 μm (the center of the cathode catalyst layer), (3: after the 20,000 ADT cycles) at Z = 30 μm (the Nafion membrane). The depth profiles of total Pt species, for fractions **A**, **B**, and **C** before and after the 20,000 ADT cycles. Cell voltage = 1.0 V. Scale = 600×600 μm. (B2: white-dashed circles) Examples of observed black parts between domains.

of the relative Pt density was defined by its maximum in the MEA. Figure 2 shows the cross-sectional images of the location and valence state of Pt at 1.0 V in **A** and **B** in the MEA (XY) plane at Z = 10 and 30 μm before and after ADT. The depth (Z) dependencies of the Pt location in the three regions are also plotted. The fraction of **C** was as low as 3-5%.

Before ADT, the fraction of **A** was estimated to be 20% of the total amount of Pt in the MEA, and Pt in **A** spread in the cathode catalyst layer (Figure 2 (A1)). After the 20,000 ADT cycles, the fraction of **A** almost unchanged, but the depth profile of **A** broadened and shifted from the cathode catalyst layer to the Nafion membrane side as shown in Figure 2. Indeed, the cross-sectional images of the Pt distribution at Z = 30 μm in the Nafion membrane widely changed after ADT. Many red domains were clearly observed in Figure 2 (A3), indicating the degradative migration and aggregation of Pt from the cathode catalyst layer to the Nafion membrane by ADT.

The fraction of Pt in **B** was 74-75% and almost unchanged during the ADT cycles. Pt in **B** mainly located inside the cathode catalyst layer before ADT. A cross-sectional image at Z = 10 μm (Figure 2 (B1)) showed that the Pt catalyst was widely distributed in domains, and its valence state at 1.0 V was found to be inhomogeneous (Figures 2 (B'1) and S6). Yellow and green parts with about +1 Pt valence state suggested that the surface of the Pt catalyst particles oxidized at 1.0 V in the parts. Blue parts with low Pt valence state were also found at the boundary of the domains.

After the 20,000 ADT cycles, remarkable changes were observed in both the location and the valence state of Pt in **B**. The depth profile of the Pt density in **B** was also shifted to the Nafion membrane area, and a plateau region was observed around a depth (Z) of 30 μm. At Z = 10 μm, which is the center of the cathode catalyst layer, Pt was still located in the body of the domains, but black parts between the domains (white-dashed circles in Figure 2 (B2)) looked expanded, indicating the dissolution of the Pt catalyst. The average Pt valence state was found to be 0.5 (Figures 2 (B'2) and S6), which was lower than that before ADT (Figure 2 (B'1)). The lower Pt valence state was observed at the entire area in the cross-sectional image, indicating that aggregation to increase the size of the Pt particle occurred in the entire cathode catalyst layer during the ADT cycles.

In contrast, at Z = 30 μm, which is the Nafion membrane area, significant appearance of Pt was observed as shown in Figure 2 (B3). Judging from the fact that the Pt amount in **B** was constant after ADT, Pt observed at Z = 30 μm was migrated from the cathode catalyst layer during ADT. The Pt valence state in **B** (Figures 2 (B'2) and (B'3)) was found to be 0.4–0.5, lower than that in Figure 2 (B'1), indicating the aggregation of the Pt catalyst by the ADT cycles. An *ex situ* SEM image measured after the *operando* CT-XANES measurements agreed with the formation of a Pt band at around Z = 30 μm (Figure S7).

The *operando* CT-XANES images suggested the degradation process of the Pt catalyst at the cathode during the ADT of PEFC. In the as-prepared MEA before ADT, although there was original heterogeneous aggregation of the Pt catalyst, which would be caused by the MEA preparation process, the major Pt component (**B**) spread to domains in the entire cathode catalyst layer. Their average Pt oxidation state (+1.1) showed by the CT-XANES image suggested that the number of surface active site was still kept on the Pt cathode catalyst at this stage (Figure S6).[8]

After the 20,000 cycles of ADT, it was found that Pt in both **A** and **B** were dissolved and migrated from the cathode catalyst layer to the Nafion membrane. The similar domain patterns of the Pt distribution images at Z = 10 and 30 μm suggested that the migration of Pt spread to the depth direction by the ADT cycles and the undesirable Pt band was formed in the Nafion membrane layer. The fact that the reduction of the Pt valence state was observed at all depth indicates that the irreversible degradative aggregation of the Pt catalyst occurred in the entire cathode catalyst layer (Figure S6), resulting in decreasing in the number of the surface active sites on the Pt cathode catalyst.[8]

The repetition of the cell-voltage operation, which is necessary for practical PEFC operation for automobiles, caused the irreversible oxidation, dissolution, migration, and aggregation of the Pt cathode catalyst in the entire cathode layer. The *operando* 3D CT-XANES images suggested that the dissolution, migration,

and degradation of the cathode catalyst tended to spread to the depth direction of the MEA.

Experimental Section

An MEA (3 × 3 cm^2) was prepared by EIWA Co. Ltd. with 50 wt % Pt/C (TEC10E50E, Tanaka Kikinzoku Kogyo K.K.; 0.5 $mg_{\text{-Pt}}$ cm^{-2}), 50 wt % Pd/C (TECPd(ONLY)E50E, Tanaka Kikinzoku Kogyo K.K.; 0.5 $mg_{\text{-Pd}}$ cm^{-2}), and a Nafion membrane (NR-212, Sigma-Aldrich). GDLs (TGP-H-030, Toray Ind., Inc.; 100 μm thick) were used. H_2 (99.99999%, supplied at anode at 150 mL min^{-1}) and N_2 (99.99999%, supplied at cathode during CT-XANES measurements at 600 mL min^{-1}), or air (99.99999%, supplied at cathode during aging at 600 mL min^{-1}) were supplied by mass-flow controllers and were bubbled through humidifiers set at a RH of 70% with a commercial gas supply kit (CNF52742, NF Co., Ltd.). The temperature of the PEFC cell was kept at 353 K. ECSA was estimated from the charge density of adsorbed/desorbed hydrogen in CV (Figure S3). The MEA was aged 150 times in 23 fixed current steps for 6 s, and ADT was performed with rectangular voltage cycling steps at 0.6–1.0 V for 3 s (Supporting Information 1).

Operando CT-XANES measurements were conducted at the BL36XU undulator beamline at SPring-8, Japan (Supporting Information 2). The PEFC cell was irradiated with X-rays monochromatized by Si(111) channel-cut crystals through a paper rotation diffuser, and the X-ray transmission images of the sample were recorded at each projection angle by a high-resolution X-ray imaging unit (AA50, Hamamatsu Photonics, K.K.) coupled with a low-noise sCMOS camera (Orca-Flash 4.0 V2, Hamamatsu Photonics, K.K.). The effective size in the image was 300 nm per pixel. The sample was rotated from -80° to 80° and 1600 projection images were recorded every 0.1° at each X-ray energy. The series of projection images ($I(E)$) was recorded at 184 energies around the Pt L_{III}-edge (11.451–11.631 keV) together with $I_0(E)$ images. The dark signal of the sCMOS camera (I_d) was extracted from the $I(E)$ and $I_0(E)$ images. The total measurement time for CT-XANES for a sample was 2.5 h (about 1 min for each X-ray energy). The CT measurements were taken under *in situ* conditions at 1.0 V. The reconstruction of the transmission images was written in Supporting Information 3.

The 3D images of the Pt distribution (**ii**) in the MEA were obtaind by the following data processing. In step 1, the series of X-ray transmission images at different X-ray energies were converted to a four-dimensional matrix (*XY*-projection coordinates, projection angle θ, X-ray energy). In step 2, absorption coefficient (μt) values in each pixel on the 2D transmission image were calculated by Beer's law. In step 3, Pt L_{III}-edge XANES spectra in each pixel in the 2D image were organized (Figure S8) and fitted with a combination of linear, arctangent, and Lorentz functions (eq. 1) to estimate the edge jump ($\boldsymbol{b_1}$) and Pt L_{III}-edge white-line height ($\boldsymbol{c_1}$) in each pixel on the 2D image. In step 4, the obtained $\boldsymbol{b_1}$ or $\boldsymbol{c_1}$ in the *XY*-projection coordinates and the projection angle θ were reconstructed into $\hat{\boldsymbol{b}}_{\boldsymbol{1}}$ or $\hat{\boldsymbol{c}}_{\boldsymbol{1}}$ in real-space *XYZ* coordinates. The 3D plot of $\hat{\boldsymbol{b}}_{\boldsymbol{1}}$ provided the 3D Pt density distribution in real space (**ii**). $\hat{\boldsymbol{c}}_{\boldsymbol{1}} / \hat{\boldsymbol{b}}_{\boldsymbol{1}}$ was converted to the absolute Pt valence state by using the white-line heights of Pt foil (Pt^0) and Pt acetylacetonate (Pt^{2+}) as standards, and the 3D distribution of Pt valence state (**iii**) was obtained (Figure S6 and Supporting Information 3).

$$\mu t = \{a_0 + a_1(E - E_0)\} + \frac{b_1}{\pi}\left\{\frac{\pi}{2} + arctan\left(\frac{E - b_2}{b_3}\right)\right\} + \frac{c_1}{1 + \left(\frac{E - c_2}{c_3}\right)^2} \qquad \text{(eq. 1)}$$

a_0, a_1, b_1, b_2, b_3, c_1, c_2, c_3: fitting constants
E: X-ray energy
E_0: edge energy at the Pt L_{III}-edge

Keywords: Computed tomography • XANES imaging • PEFC • catalyst degradation • Pt cathode catalyst

[1] a) M. Z. Jacobson, W. G. Colella, D. M. Golden, *Science*, **2005**, *308*, 1901; b) A. Kongkanand, M. F. Mathias, *J. Phys. Chem. Lett.*, **2016**, *7*, 1127; c) M. K. Debe, *Nature*, **2012**, *486*, 43.

[2] a) A. Rabis, P. Rodriguez, T. J. Schmidt, *ACS Catal*., **2012,** *2*, 864; b) F. A. de Bruijn, V. A. T. Dam, G. J. M. Janssen, *Fuel Cells*, **2008**, *8*, 3.

[3] a) X. Wang, M. Vara, M. Luo, H. Huang, A. Ruditskiy, J. Park, S. Bao, J. Liu, J. Howe, M. Chi, Z. Xie, Y. Xia, *J. Am. Chem. Soc*., **2015**, *137*, 15036; b) K. Nagasawa, S. Takao, S. Nagamatsu, G. Samjeské, O. Sekizawa, T. Kaneko, K. Higashi, T. Yamamoto, T. Uruga, Y. Iwasawa, *J. Am. Chem. Soc.*, **2015**, *137*, 12856; c) W. Schmittinger, A. Vahidi, *J. Power Sources*, **2008**, *180*, 1; d) J. Yu, T. Matsuura, Y. Yoshikawa, M. N. Islam, M. Hori, *Electrochem. Solid-State Lett.*, **2005**, *8*, A156; e) J. Xie, D. L. Wood, D. M. Wayne, T. A. Zawodzinski, P. Atanassov, R. L. Borup, *J. Electrochem. Soc.*, **2005**, *152*, A104.

[4] a) J. C. Meier, C. Galeano, I. Katsounaros, A. A. Topalov, A. Kostka, Ferdi Schüth, K. J. J. Mayrhofer, *ACS Catal.*, **2012**, *2*, 832; b) J. Xie, D. L. Wood, K. L. More, P. Atanassov, R. L. Borup, *J. Electrochem. Soc.*, **2005**, *152*, A1011.

[5] a) S. Takao, O. Sekizawa, S. Nagamatsu, T. Kaneko, T. Yamamoto, G. Samjeské, K. Higashi, K. Nagasawa, T. Tsuji, M. Suzuki, N. Kawamura, M. Mizumaki, T. Uruga, Y. Iwasawa, *Angew. Chem. Int. Ed.*, **2014**, *53*, 14110; b) K. Sasaki, N. Marinkovic, H. S. Isaacs, R. R. Adzic, *ACS Catal.*, **2016**, *6*, 69; c) K. Nagasawa, S. Takao, K. Higashi, S. Nagamatsu, G. Samjeské, Y. Imaizumi, O. Sekizawa, T. Yamamoto, T. Uruga, Y. Iwasawa, *Phys. Chem. Chem. Phys.*, **2014**, *16*, 10075; d) B. Bozzini, M. K. Abyaneh, M. Amati, A. Gianoncelli, L. Gregoratti, B. Kaulich, M. Kiskinova, *Chem. Eur. J.*, **2012**, *18*, 10196.

[6] a) K. Malek, A. A. Franco, *J. Phys. Chem. B*, **2011**, *115*, 8088; b)S. G. Rinaldo, W. Lee, J. Stumper, M. Eikerling, *Electrochem. Solid-State Lett.*, **2011**, *14*, B47; c) A. A. Franco, M. Gerard, *J. Electrochem. Soc.*, **2008**, *155*, B367.

[7] a) C. G. Chung, L. Kim, Y. W. Sung, J. Lee, J. S. Chung, *Int. J. Hydrogen Energy*, **2009**, *34*, 8974; b) X. G. Yang, Y. Tabuchi, F. Kagami, C. Y. Wang, *J. Electrochem. Soc.*, **2008**, *155*, B752.

[8] a) N. Ishiguro, S. Kityakarn, O. Sekizawa, T. Uruga, H. Matsui, M. Taguchi, K. Nagasawa, T. Yokoyama, M. Tada, *J. Phys. Chem. C*, **2016**, *120*, 19642; b) S. Kityakarn, T. Saida, A. Sode, N. Ishiguro, O. Sekizawa, T. Uruga, K. Nagasawa, T. Yamamoto, T. Yokoyama, M. Tada, *Topics Catal*., **2014**, *57*, 903.

[9] a) J. Wang, Y. K. Chen-Wiegart, C. Eng, Q. Shen, J. Wang, *Nat. Commun.*, **2016**, *7*, 12372; b) F. Meirer, D. T. Morris, S. Kalirai, Y. Liu, J. C. Andrews, B. M. Weckhuysen, *J. Am. Chem. Soc.*, **2015**, *137*, 102; c) S. W. T. Price, K. Geraki, K. Ignatyev, P. T. Witte, A. M. Beale, J. F. W. Mosselmans, *Angew. Chem. Int. Ed.*, **2015**, *54*, 9886; d) H. E. van der Bij, D. Cicmil, J. Wang, F. Meirer, F. M. F. de Groot, B. M. Weckhuysen, *J. Am. Chem. Soc*., **2014**, *136*, 17774.; e) P. Senecal, S. D. M. Jacques, M. Di Michiel, S. A. J. Kimber, A. Vamvakeros, Y. Odarchenko, I. Lezcano-Gonzalez, J. Paterson, E. Ferguson, A. M. Beale, *ACS Catal.*, **2017**, *7*, 2284; (f) M. E. Birkbak, I. G. Nielsen, S. Frølich, S. R. Stock, P. Kenesei, J. D. Almer, H. Birkedal, *J. Appl. Cryst.*, **2017**, *50*, 192; (g) M. Álvarez-Murga, P. Bleuet, J.-L. Hodeau, *J. Appl. Cryst.*, **2012**, *45*, 1109; (h) F. Vanmeert, G. Van de Snickt, K. Janssens, *Angew. Chem. Int. Ed.*, **2015**, *54*, 3607; (i) V. Berejnov, D. Susac, J. Stumper, A. P. Hitchcock, *ECS Trans*., **2012**, *50*, 361.

[10] T. Saida, O. Sekizawa, N. Ishiguro, M. Hoshino, K. Uesugi, T. Uruga, S. Ohkoshi, T. Yokoyama, M. Tada, *Angew. Chem. Int. Ed.*, **2012**, *51*, 10311.

[11] M. Tada, T. Uruga, Y. Iwasawa, *Catal. Lett.*, **2015**, *145*, 58.

[12] a) P. A. Midgley, R. E. Dunin-Borkowski, *Nature Mater.*, **2009**, *8*, 271; b) D. Verhoeven, *Appl. Opt.*, **1993**, *32*, 3736.

WILEY-VCH

Entry for the Table of Contents (Please choose one layout)

COMMUNICATION

3D Visualization of Fuel Cell Catalyst Degradation:

The 3D distribution and oxidation state of a Pt cathode catalyst in a practical MEA were visualized under PEFC operating conditions. *Operando* 3D CT-XANES technique clearly revealed the heterogeneous migration and degradation of the Pt cathode catalyst in the MEA during ADT cycles.

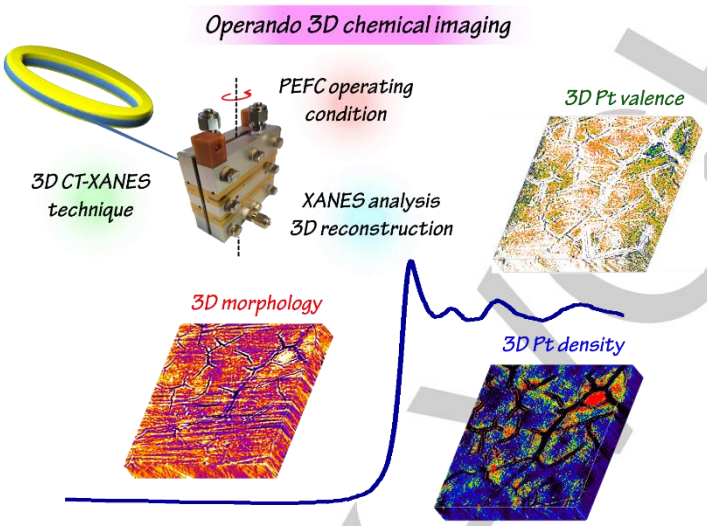

H. Matsui, N. Ishiguro, T. Uruga, O. Sekizawa, K. Higashi, N. Maejima, and M. Tada

Page No. – Page No.

***Operando* 3D Visualization of Migration and Degradation of Pt Cathode Catalyst in a Polymer Electrolyte Fuel Cell**

WILEY-VCH